

# The Effect of Erosion on Corrosion Protection Properties of Coal Tar Epoxy Coating

M. Atapour <sup>1\*</sup>, S. Abdollahi <sup>2</sup>, S. M. Monir Vaghefi <sup>3</sup>

<sup>1,2,3</sup> Department of Materials Engineering, Isfahan University of Technology, Isfahan 84156-83111, Iran

## Abstract

In this work, the effect of erosion on corrosion behavior of coal tar epoxy coating was evaluated using electrochemical impedance spectroscopy (EIS) measurements. The surface morphology of the coating was examined by scanning electron microscope (SEM) after 10, 20, 30, 45 and 60 min of erosion process at an impact angle of 90°. After 10 min of erosion process, the Nyquist plots showed just a single large capacitive semicircle and the phase Bode plots exhibited a line close to  $-80^\circ$  in the middle-frequency region, thereby indicating high corrosion resistance (about  $109 \Omega\text{cm}^2$ ). After 20 and 30 min of erosion process, the diameter of the Nyquist semicircle was decreased with time and two semicircles appeared after 45 min. Furthermore, SEM observations revealed that the protection performance of coating was decreased by an increase in time of erosion due to the formation of holes and electrolyte penetration into the coating. Finally, after 60 min of erosion process, the coating was partially removed and the substrate appeared.

**Keywords:** Erosion, Electrochemistry, Coal tar coatings, Surface morphology, EIS.

## 1. Introduction

The use of organic coatings is highly effective in corrosion protection of steel structures. These coatings have been widely used in various marine applications where aggressive media are involved, such as pipelines, storage tanks, ships, bridges and the equipment of desalination plants <sup>1-3</sup>. In several applications, such as offshore structures, hydraulic turbines, slurry pumps, pipelines and agitators, organic coatings need to exhibit not only good protection properties and aesthetic appearance, but also an improved resistance to impact and erosion. Under erosion conditions, the protection properties of many protective coatings are extremely vulnerable to impact damages <sup>4,5</sup>.

Generally, erosion-corrosion (E-C) process occurs when a material is exposed to a flowing liquid. In this condition, the rate of degradation is higher than those caused by pure corrosion or pure erosion individually due to their synergistic effects <sup>6</sup>. It has been demonstrated that the synergism effects of corrosion and erosion processes can be reduced by using organic or ceramic protective coatings <sup>7,8</sup>. The organic coatings offer excellent resistance to corrosion in general, but

they can be susceptible to damage in erosion conditions <sup>9</sup>. Thus, the study of erosion-corrosion resistance of organic coatings is very important for some applications.

Today, different industries such as power plants and the offshore oil and gas infrastructures have been developed extensively in the marine environments, such as that in the Persian Gulf region. However, the growing scarcity of freshwater is one of the main threats for the long term activity of energy industries. In this situation, the use of seawater is recognized as the main water source and can become a vital alternative for energy industries.

Under the prevailing condition of Persian Gulf environment, the use of coatings for the prevention of corrosion is practiced widely. The use of coal tar coatings was stopped in Europe in 1990 due to health concerns. However, coal tar epoxies are still among the most commonly used corrosion resistant coatings in Persian Gulf region <sup>10</sup>. These coatings exhibit high degrees of corrosion and humidity protection. Thus, it is well accepted that the coal tar epoxy coatings can provide excellent resistance to salty water, fresh water, mild acids and mild alkalis. Low water permeability, high corrosion resistance, good adhesion and the low cost of coal tar epoxy coatings have contributed to their noticeable applications in different marine industries <sup>10,11</sup>.

It has been widely accepted that the electrochemical

\* Corresponding author

Tel: +98 31 33915735

Email: m.atapour@cc.iut.ac.ir

Address: Department of Materials Engineering, Isfahan University of Technology, Isfahan 84156-83111, Iran

1. Assistant Professor

2. M.Sc.

3. Associate Professor

impedance spectroscopy (EIS) is a powerful technique for the investigation of degradation phenomena taking place at organic coated substrates<sup>12)</sup>. EIS makes it possible to obtain electrochemical elements such as coating capacitance, coating resistance, double layer capacitance and charge transfer resistance related to corrosion reactions. Determination of these elements is very useful to assess the protective performance of organic coatings<sup>10-14)</sup>.

Valentini et al.<sup>15)</sup> studied the corrosion behavior of coal tar epoxy coatings using EIS and electrochemical noise methods. A decrease in the corrosion resistance of the coating with increasing the exposure time resulted from the use of these two methods<sup>15)</sup>. Zhang et al.<sup>16)</sup> evaluated the protective performance of coal tar epoxy coatings with different amounts of titanium powder by using EIS. It was found that different amounts of the Ti powder changed the permittivity of the coatings with time.

As it is well established, erosion-corrosion is a severe and complicated challenge in oil and gas industry. Therefore, the detailed study of the erosion-corrosion behavior is important. The application of coal tar epoxy coating seems to be classical or old work. However, due to the excellent resistance of this coating in saltwater, freshwater, mild acids and mild alkalies, its use has continued in recent years. Accordingly, there have been published papers regarding electrochemical evaluations of this coating<sup>15)</sup>. A literature survey showed that the erosion-corrosion behavior of coal tar epoxy coating has been less studied. Thus, our new study attempted to evaluate the erosion-corrosion behavior of this coating. Thus, our new study evaluated the erosion-corrosion behavior of this coating. In this study, the erosion-corrosion behavior of coal tar epoxy coating applied to a carbon steel substrate was investigated using a high pressure liquid-gas jet with solid particles of  $\text{SiO}_2$ .

## 2. Material and Methods

Carbon steel specimens with the dimensions  $40 \times 40 \times 4 \text{ mm}^3$  were sand blasted with  $\text{SiO}_2$  sand. Coal tar epoxy was applied by brush and cured for two weeks at room temperature. Coal tar epoxy was a commercially available epoxy resin (E20) modified with coal tar. Polyamine was used as the curing agent in this compound. The final thickness of the applied coating was about  $210 \mu\text{m}$  as measured with a micrometer based on ASTM D1005/95.

According to our investigations, erosion-corrosion is one of the common types and possible causes of deterioration process of coal tar coatings. Fig. 1 shows one of the coatings applied to protect the interior surface of a pipe used in a cooling tower system in Persian Gulf region.

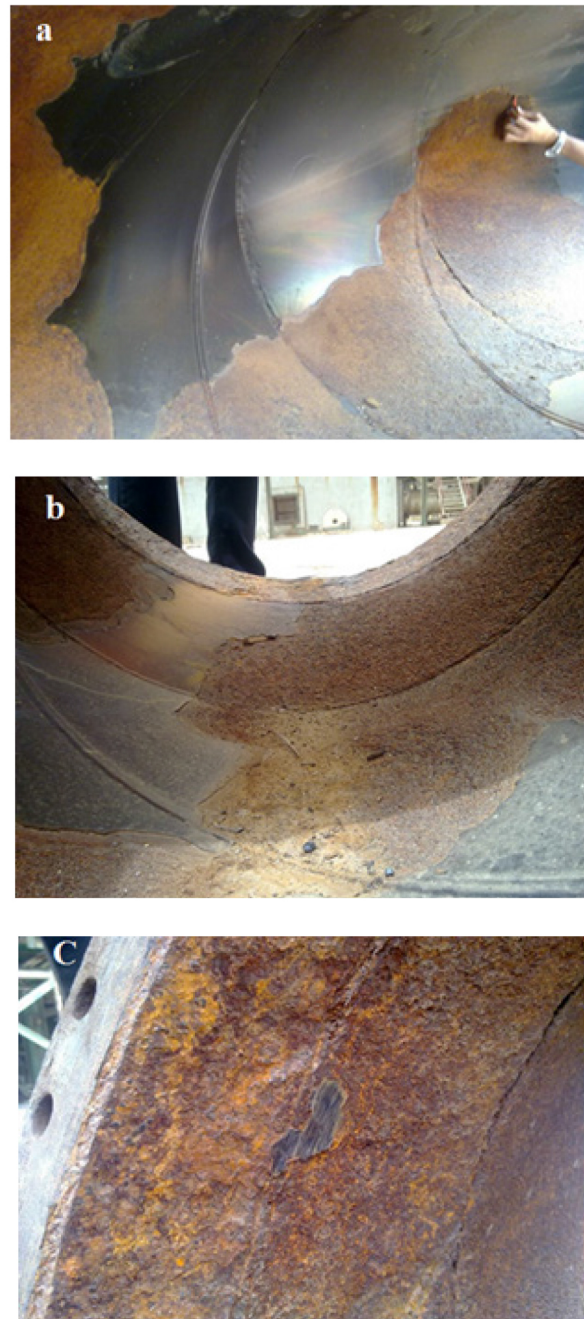


Fig. 1. (a) Close-up view of an interior surface of a pipe used in a cooling tower system in the coast of Persian Gulf (The Razi Petrochemical Co.), (b) the Coal tar coating was deteriorated due to erosion-corrosion after 3 years, and (c) severely-damage areas.

This coal tar coating was deteriorated after 3 years of exposure to seawater due to erosion-corrosion. Weight-loss measurements and electrochemical impedance spectroscopy combined with scanning electron microscopy (SEM) observations were used to evaluate the erosion-corrosion resistance of the coating. The results of this investigation can assist the development of various marine industries

including oil and water pipes, desalination plants services, power plant cooling systems as well as different pipelines and tanks.

Erosion experiments were performed using a high pressure liquid-gas jet with solid particles of  $\text{SiO}_2$ . A schematic diagram of the apparatus is presented in Fig. 2. The output nozzle with a bore of 6 mm was made of stainless steel. In the reservoir, water and silica sand were continually mixed with a stirrer. The sand was sieved for 5 min using a mechanical shaker and only particles with a size range of 100-150  $\mu\text{m}$  were used.

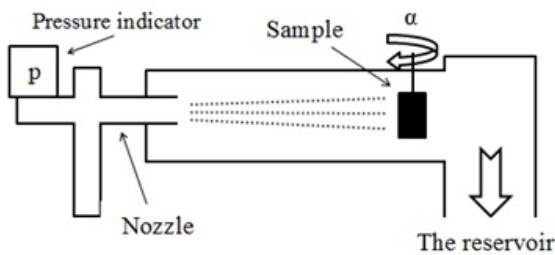


Fig. 2. Schematic diagram of erosion test apparatus.

By circulating the gas through the loop, the mixture of water and silica sand was sprayed over the specimen for 60 min. The impact angle of solid particles was  $90^\circ$ . It should be mentioned that erosion-corrosion tests were also carried out at impact angles of  $30^\circ$  and  $60^\circ$ . However, it seemed that the presentation of all results could be complicated for readers. Thus, in this work, the results of erosion-corrosion tests obtained at the impact angle of  $90^\circ$  have been presented.

The sand concentration and mean impact velocity were 3.0 wt% and  $30 \text{ m s}^{-1}$ , respectively. These parameters were selected to intensify the erosion and reduce the time of experiments. In erosion tests, the distance between the specimen and the output nozzle was 20 cm. The feed pressure of 3.5 bar was selected in the present study.

The specimens were rinsed with distilled water before and after erosion test. In order to avoid the effect of moisture, the samples were dried at  $50^\circ\text{C}$  for 60 min and then cooled down to room temperature before weighing. To evaluate the damage, the total mass loss was measured using a balance with a tolerance of  $\pm 0.1 \text{ mg}$ . The morphology of the coatings was evaluated by SEM before and after erosion processes at different times. Philips XL 30 scanning electron microscope (SEM) was used in this investigation. The analyses were conducted with an operating voltage of 20 kV, a spot size of 3 and a working distance of 5 mm. In order to obtain more detailed information about the corrosion behavior of the weld, we assessed the protective performance of coatings.

In order to obtain more detailed information about the protective performance of the coating, electrochemical measurements were also carried out. The influence of erosion on the corrosion properties of the coating was evaluated using EIS measurements with a PARSTAT 2273 potentiostat. The EIS test solution was 3.5 wt% NaCl with a signal amplitude of 20 mV and a frequency range of 100 kHz to 10 mHz at the open circuit potential (OCP). A platinum electrode and an Ag/AgCl KCl saturated were used as counter (auxiliary) and reference electrodes, respectively. The exposed surface area was about  $7.6 \text{ cm}^2$ .

### 3. Results and Discussion

The SEM image of the  $\text{SiO}_2$  particles used in this investigation is shown in Fig. 3. It can be seen that the particle sizes were in the range of 100-150  $\mu\text{m}$ .

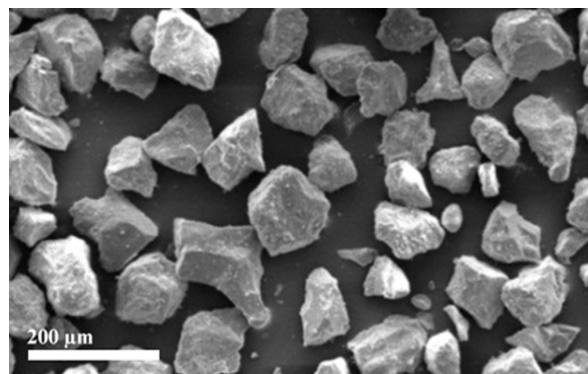


Fig. 3. SEM images of the sand particles used as erosion particles.

Fig. 4 depicts the total mass loss of the coating as a function of erosion time. As shown in Fig. 4, an incubation period (stage I from 0 to 15 min) was observed in the total mass plot, where there was no appreciable weight loss. In stage II from 15 to 40 min (acceleration period), the rate of material removal was maximum. After a critical time (about 40 min), in stage III, called attenuation period, the erosion rate began to decrease to a constant lower rate because of the total destruction of the coating and the substrate direct exposure to the erosion particles.

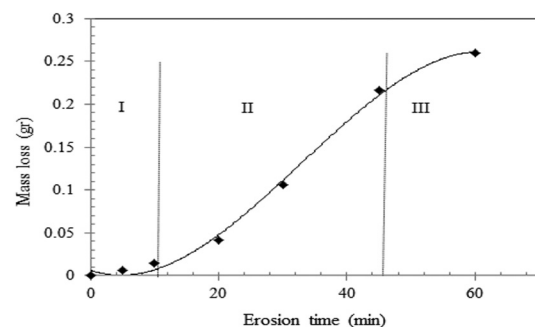


Fig. 4. Coating weight loss as a function of erosion time.

During the erosion process, water containing sand impacts led to the diffusion of electrolyte into the substrate surface due to the formation of defects on the coating. This process decreased the corrosion resistance of the coating. Fig. 5 shows the microstructure of the coating before and after erosion. At impact angle of  $90^\circ$ , the erosion was dominated by plastic deformation and propagation of defects (Fig. 5c). In other words, recurrent impacts of erodent particles at the angle of  $90^\circ$  caused the loosening of a piece of the coating from the impact site<sup>18-20</sup>. After 60 min of erosion process, the coating was partially removed and the substrate appeared (Fig. 5d).

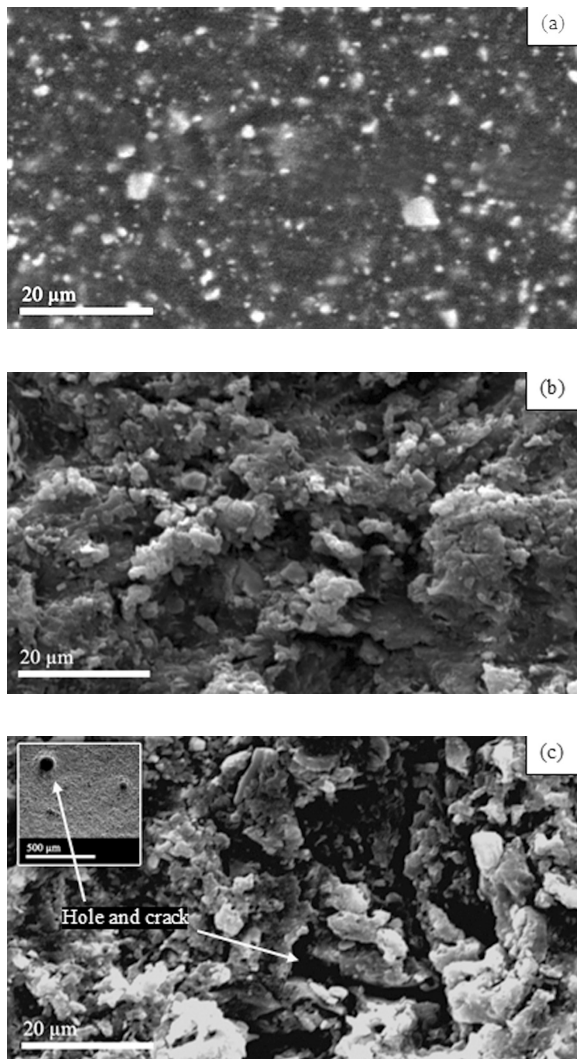


Fig. 5. The coating SEM micrographs (a) before and after; (b) 30 min, (c) 45 min, and (d) 60 min erosion process with a  $90^\circ$  impact angle.

Nyquist and Bode plots of the coated specimens after 10 min of the erosion experiment are shown in Fig. 6. Nyquist plot showed a huge semicircle and the Bode plot represented a capacitance behavior, implying the high corrosion resistance of the coating. The impedance modulus  $|Z|$  at low frequencies

displayed very large values ( $>10^9 \Omega \text{ cm}^2$ ). The slope of  $Z-\log f$  curve was about  $-1$  and the phase angle was almost  $-80^\circ$  (Figs. 6b and 6c). A time constant could be observed from the impedance spectra responsible for the barrier characteristic of the coal tar epoxy coating<sup>12, 13</sup>. After 10 min, coating capacitance ( $C_c$ ) and pore resistance ( $R_{\text{por}}$ ) were about  $3.1 \times 10^{-10} \text{ F cm}^{-2}$  and  $1.5 \times 10^{+9} \Omega \text{ cm}^2$ , respectively. These data were related to the as-received coating, which had a very high corrosion resistance.

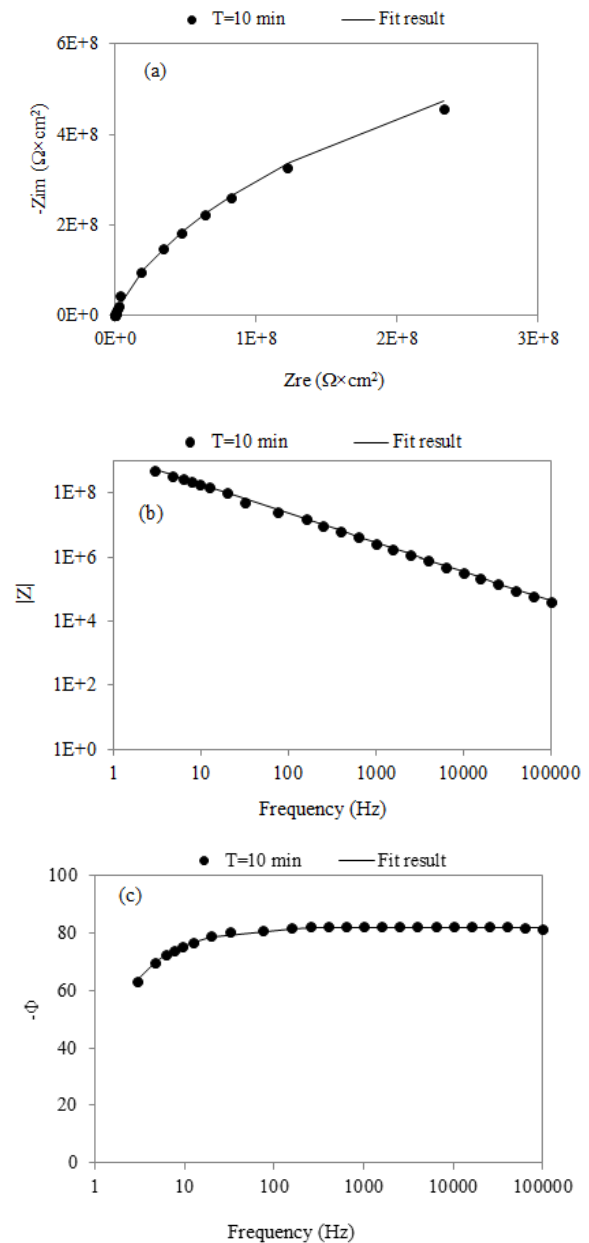


Fig. 6. Impedance diagrams of samples after 10 min erosion process in the form of (a) Nyquist, (b) Bode, and (c) Bode phase plots.

When an ionic path was created in the coating, a depressed semi-circle was generally observed in the Nyquist plot that could be represented by an electrical

equivalent circuit including the solution resistance  $R_s$  in series with a parallel combination of the coating capacitance  $C_c$  and the film resistance  $R_p$  (Fig. 7a). It must be noted that ordinary capacitors were often replaced with constant phase elements (CPE) in order to consider the divergence from the pure capacitive behavior. The pore resistance,  $R_{por}$ , was an indication of the opposition to the penetration of aggressive ions and therefore, was related to the corrosion properties of the coatings<sup>15</sup>.

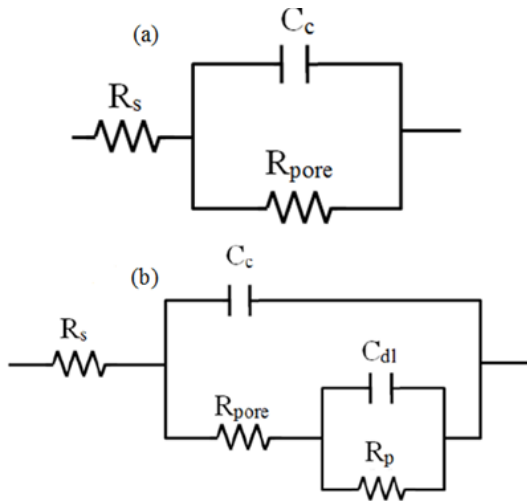


Fig. 7. Electrical equivalent circuits for Nyquist plots with (a) one and (b) two time constants. These circuits consist of  $R_s$ : solution resistance,  $C_c$ : coating capacitance,  $R_p$ : film resistance,  $C_{dl}$ : double layer capacitance, and  $R_{por}$ : pore resistance.

Figs. 8 and 9 indicate Nyquist and Bode plots of coal tar epoxy coating in 3.5% NaCl solution with an erosion time of 60 minutes. As observed, the impedance modulus  $|Z|$  at the low frequencies was decreased with erosion time, showing that the coating specimens suffer a degradation process after erosion. It seemed that the electrolyte penetration through the coating and creation of a path to the substrate surface due to the erosion damages were the source of deterioration.

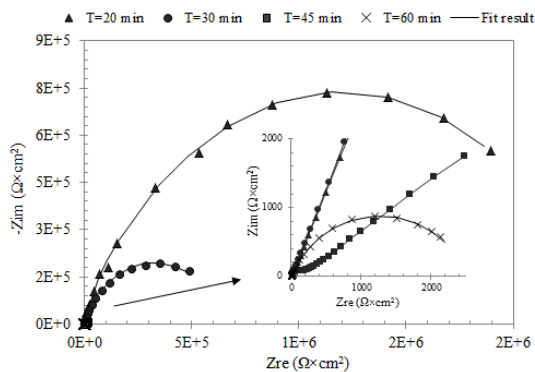


Fig. 8. Nyquist plots of coal tar epoxy coating in 3.5% NaCl solution in different erosion test times.

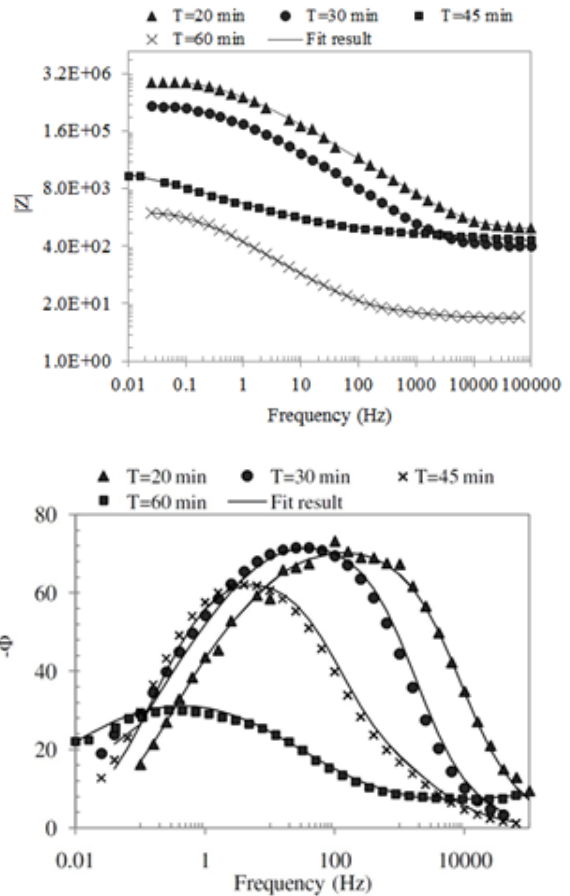


Fig. 9. Bode plots of coal tar epoxy coating in 3.5 wt. % NaCl solution in different erosion times.

However, as the erosion time was expired, the frequency range displaying a capacitive behavior in the Bode phase plots was decreased and this was more pronounced for the coating applied on carbon steel. At the same time, a decrease in the values of the impedance modulus  $|Z|$  to the values in the range of  $10^4$ – $10^7$   $\Omega\text{cm}^2$  occurred at the high frequencies, indicating that the coating was an imperfect dielectric. The expansion in the second time constant of the impedance diagrams finally occurred at longer erosion times (45 min) and it could be detected by the second semicircle in the Nyquist diagrams at the lower frequencies. At this state, the barrier properties of the coating were totally absent in certain areas and the substrate was directly exposed to the solution. Hence, the first semicircle was related to the barrier characteristics of the as-received coating and the second one described the corrosion process occurring at the substrate/coating interface in the defective areas of the coating, specifically the charge transfer process between the substrate and the solution. Under these conditions, the electrical equivalent circuit was given by Fig. 7b. In this circuit, a capacitor,  $C_{DL}$ , accounted for the spread of ionic charges near the unprotected substrate, and a resistor,  $R_{ct}$ , which was inversely

commensurate with the corrosion rate of the specimen<sup>13-15</sup>, was also used.

At erosion time of 45 min, a breakdown in the coating occurred with the development of defects, resulting in significantly smaller impedance values ( $<10^6 \Omega\text{cm}^2$ ) in all frequency ranges. The pore resistance,  $R_{\text{por}}$ , is an important element for the evaluation of corrosion resistance of the coating and the coating capacitance  $C_C$  is related to the presence of the coating<sup>17,18</sup>. During the diffusion of the solution into the coating, the dielectric constant of coating was changed and thus,  $C_C$  was altered too. The logarithm of coating capacitance and coating resistance was plotted as a function of erosion time (Fig. 10).

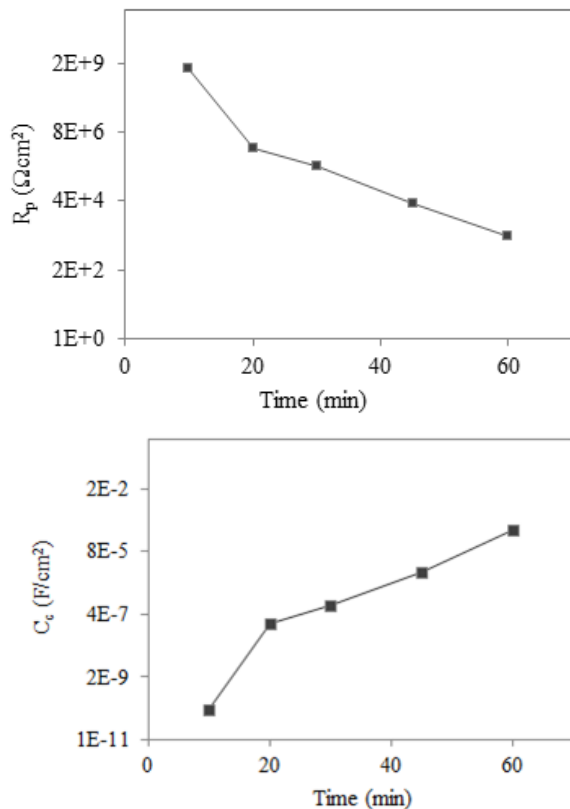


Fig. 10. Erosion time dependence of  $R_C$  and  $C_C$  of the coating.

It could be clearly observed in Fig. 10 that  $R_{\text{por}}$  was decreased and coatings capacitance  $C_C$  was increased during the erosion process. The values of coating resistance were dramatically decreased after 20 min, but after that, a small decrease occurred. The variation of  $C_C$  and  $R_{\text{por}}$  indicated that the electrolyte penetration into the coatings took place at that time. These results demonstrated that coating porosity and defect were gradually increased as the erosion process was continued.

#### 4. Conclusions

The correlation between erosion time and erosion rate showed three stages: the incubation, the acceleration and the attenuation periods. SEM observations revealed defects formation in the coating at the impact angle of  $90^\circ$  and the erosion was identified by plastic deformation. In other words, repeated impacts of erodent particles at the angle of  $90^\circ$  caused the loosening of the coating in the impact site. After 10 min of the erosion process, Nyquist plot showed a huge semicircle and the Bode plot indicated a capacitance behavior, meaning the high corrosion resistance of coating (about  $10^9 \Omega\text{cm}^2$ ). After 20 and 30 min, Nyquist semicircle shrank and turned into two semicircles after 45 min. In fact, the electrolyte penetrated into the coating, leading to a significant decrease in the corrosion resistance of the coating.

#### References

- [1] S. P. Sitaram, J. O. Stoffer, and T. J. O'Keefe: J. Coat. Technol., 69(1997), 65.
- [2] Y. Gonzalez-Garcia, S. Gonzalez, and R.M. Souto: Corros. Sci., 49 (2007), 3514.
- [3] R.I. Trezona, I.M. Hutchings: Prog. Org. Coat., 41 (2001), 85.
- [4] R.J.K. Wood: Mater. Design., 20(1999), 179.
- [5] E. Bardal, Corrosion and Protection, Second ed., Springer, London, 2004.
- [6] G.A. Zhang, L.Y. Xu, Y.F. Cheng: Corros. Sci., 512 (2009), 283.
- [7] M. Grundwurm, O. Nuyken, M. Meyer, J. Wehr, N. Schupp: Wear 263 (2007), 318.
- [8] A. Levy: Surf. Coat. Technol., 1 (1998), 387.
- [9] E. Scrinzi, S. Rossi and F. Deflorian: Surf. Coat. Technol., 203 (2009), 2974.
- [10] A. Husain, O. Al-Shamali, A. Abduljaleel: Desalination 166 (2004), 295.
- [11] E. Akbarinezhad, F. Rezaei, J. Neshati: Prog. Org. Coat., 61 (2008), 45.
- [12] R. C. Bacon, J. Smith and F. M. Rugg: Industrial & Engineering Chemistry., 40(1948), 161.
- [13] L. Jianguo, G. Gaoping, and Y. Chuanwei: Electrochim. Acta., 50 (2005), 3320.
- [14] M. Kendig, J. Scully: Corrosion., 46 (1999), 22.
- [15] C. Valentini, J. Fiora, G. Ybarra: Prog. Org. Coat. 73 (2012), 173.
- [16] X. Zhang, F. Wang, Y. Du: Prog. Org. Coat., 53 (2005), 302.
- [17] H. Marchebois, M. Keddamb, C. Savalla: Electrochim. Acta., 49 (2004), 1719.
- [18] A. Suresh, A.P. Harsha, M.K. Ghosh: Wear., 267 (2009), 1516.